Journal of Nepal Geological Society, 2013, Vol. 46, pp. 95-110

Petrography of Miocene Siwalik Group sandstones, Karnali River section, Nepal Himalaya: Implications for source lithology and tectonic setting

***Ashok Sigdel and Tetsuya Sakai**

Department of Geoscience, Shimane University, Matsue 690-8504, Japan
*(*Email: ashoksigdel7@yahoo.com)*

ABSTRACT

The Siwalik Group constitutes an important archive of Himalayan uplift and related climate changes. Compositional and textural properties of Siwalik sandstones are important parameters for the reconstruction of source lithology, uplift, and the unroofing history of the Himalaya. This study examines fluvial sandstones of the Siwalik Group along the Karnali River, where the large paleo-Karnali River is expected to have flowed. Modal QFL analysis shows that the sandstones are mainly sub-litharenites or litharenites. Multivariate statistical analysis using Principal Component Analysis (PCA) and the Weltje method show slight variations in sediment composition occur between the Chisapani and Baka Formations. These variations are mainly linked to the source area and tectonics rather than to facies, grain size, or climate. The detrital modes of the sandstones indicate recycled orogen provenance. Comparison of the detrital modes with previous studies indicates that the Higher Himalaya and Lesser Himalaya zones were a common source area throughout the time of deposition. However, subtle changes in feldspar and biotite contents indicate significant supply of detritus derived from the Higher Himalaya after 9.6 Ma.

Key words: Siwalik Group, Karnali River, Petrography, Sediment provenance, Multivariate statistics

Received: 15 April, 2013 **Revision accepted**: 31 May, 2013

INTRODUCTION

Sandstone compositions are influenced by the composition of the source rocks, the nature of the sedimentary processes operating, and the types of dispersal paths that link the source and the depositional basin (Dickinson and Suczek 1979). The provenance of sediments includes all aspects of the source area, including the source rocks present, climate, relief, and hydrodynamics of the depositional environment (Pettijohn et al. 1987; Johnsson 1993). Tectonic setting is also regarded as a major controlling factor for the variations in composition of sedimentary rocks (Ingersoll and Suczek 1979; Dickinson 1985; Johnsson 1993).

The minerals occurring in sedimentary rocks are generally used as guides for the identification of provenance and tectonic setting of an area. The most commonly used approach in provenance studies is to consider sandstone composition in the context of a tectonic framework. Standard methods for sandstone provenance analysis use modal analysis of detrital framework components (Dickinson and Suczek 1979; Dickinson 1985). Such methods have been used to determine the provenance of the fluvial succession of the Siwalik Group, which is an important repository recording the provenance and tectonic history of the Himalaya (Critelli and Ingersoll 1994).

The present study targets the Siwalik Group along the Karnali River area of Nepal Himalaya (Fig. 1). A variety of studies in this geologic section have focused on isotopes and age dating, to understand the regional tectonics, exhumation, and the provenance of the sediments (Gautam and Fujiwara 2000; Huyghe et al. 2001, 2005, Szulc et al. 2006; Van der Beek et. al. 2006; Bernet et al. 2006). Despite these isotopic and chronological studies, no detailed petrographic information is yet available for the Karnali River section. The aim of our present study is to describe the petrography of Siwalik sandstones from the Karnali River section in detail, and determine their provenance. We also examine the factors controlling the variations in sediment composition, based on multivariate statistical analysis.

GEOLOGICAL SETTING

The Siwalik Group comprises a 16.0 Ma succession of synorogenic sediments derived from the main Himalayan Range (Gansser 1964; Upreti and Le Fort 1999). The Siwalik sediments are bounded by the Main Boundary Thrust (MBT) and Main Frontal Thrust (MFT), which separates the group

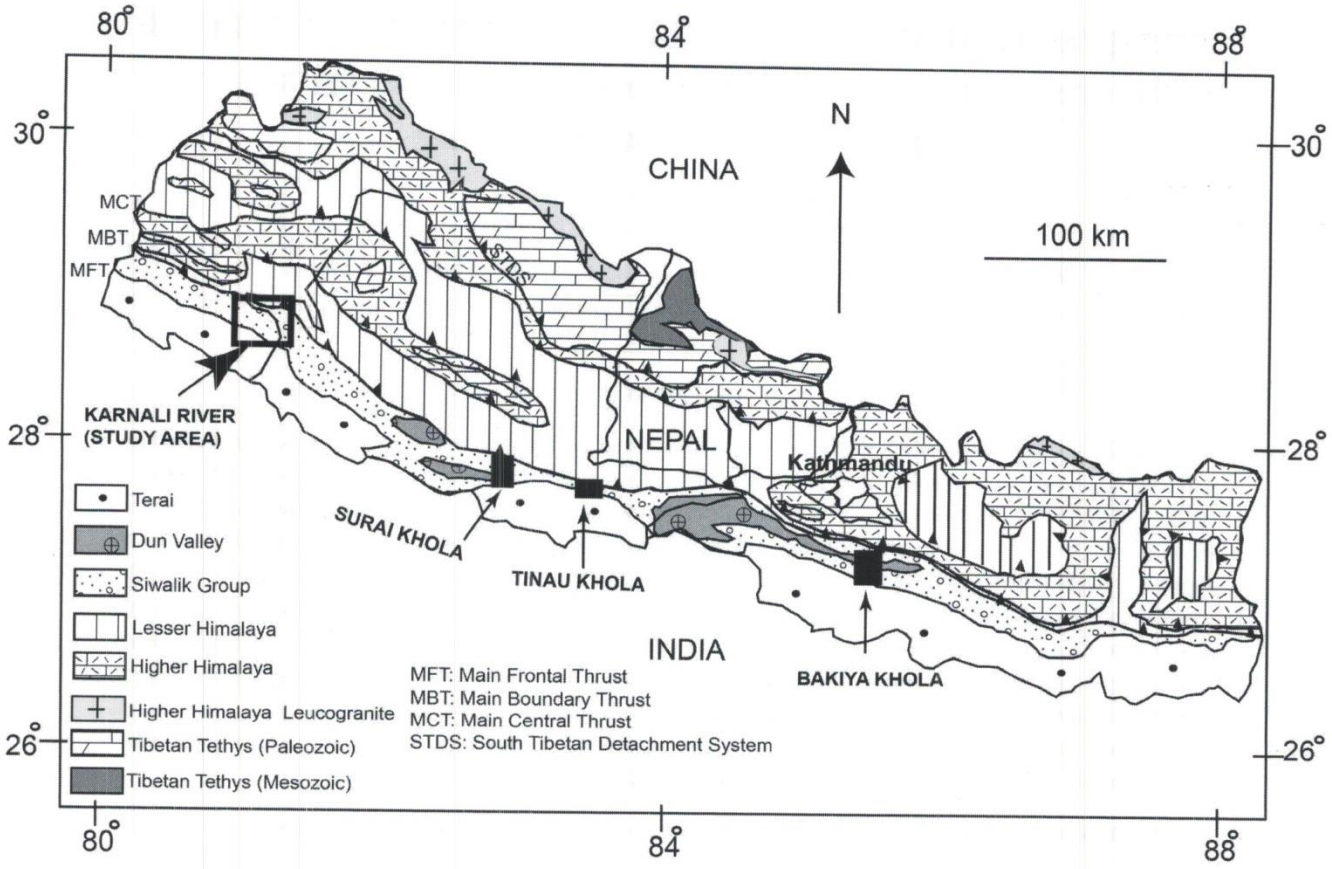

Fig. 1: Generalized geological map of Nepal Himalaya (modified from Amatya and Jnawali 1994). Open rectangle indicates the location of the study area; filled rectangles are other study area.

from the Lesser Himalaya to the north and Indo-Gangatic Plain to the south, respectively (Mugnier et al. 1999). The succession ranges from 4 to 6 km in thickness.

This study targets the Siwalik Group exposed around the Karnali River (Fig 1). The traditional tripartite lithological division (Lower, Middle and Upper Siwaliks) was previously applied (DMG 1987, 2003; Mugnier et al. 1998, 1999) for the group in this area. The age of the Karnali section ranges from 15.8 to 5.2 Ma, as obtained from paleomagnetic data (Gautam and Fujiwara 2000). Structurally, the section consists of two large belts separated by the Main Dune Thrust (MDT), an extensive and major intra-Siwalik thrust (Mugnier et al. 1999).

Sigdel et al. (2011) recently established the stratigraphy of the southern belt in this area, dividing the succession into the Chisapani Formation (equivalent to the Lower Siwaliks, 2045 m in thickness), the Baka Formation (equivalent to the Middle Siwaliks, 2740 m), and the Kuine and Panikhola Gaun Formations (equivalent to the Upper Siwaliks, 1500 m), in ascending order (Fig. 2). The Chisapani Formation is composed of red mudstones and fine- to medium-grained sandstones, and is subdivided into lower, middle, and upper members. The Baka Formation is composed of medium- to coarse-grained sandstones ("salt and pepper"), pebbly sandstones, and interbedded greenish-grey mudstones. The Baka Formation is also subdivided into lower, middle, and upper members. The Kuine Formation consists of clast-supported and imbricated pebble to cobble conglomerates, whereas the Panikhola Gaun Formation consists of thick matrix-supported pebble, cobble and boulder conglomerates.

METHODOLOGY

Point count methodology

Forty-eight sandstone samples from Karnali River Siwalik Group were selected for petrographic analysis. Of these, 26 samples were from the Chisapani Formation, and 22 from the Baka Formation (Table 1). Point counting was carried out to identify individual grain or crystals larger than 0.0625 mm, using the Gazzi-Dickinson method (Zuffa 1985). A total of 500 grains were counted for each thin section, using a Swift point counter. The framework constituents

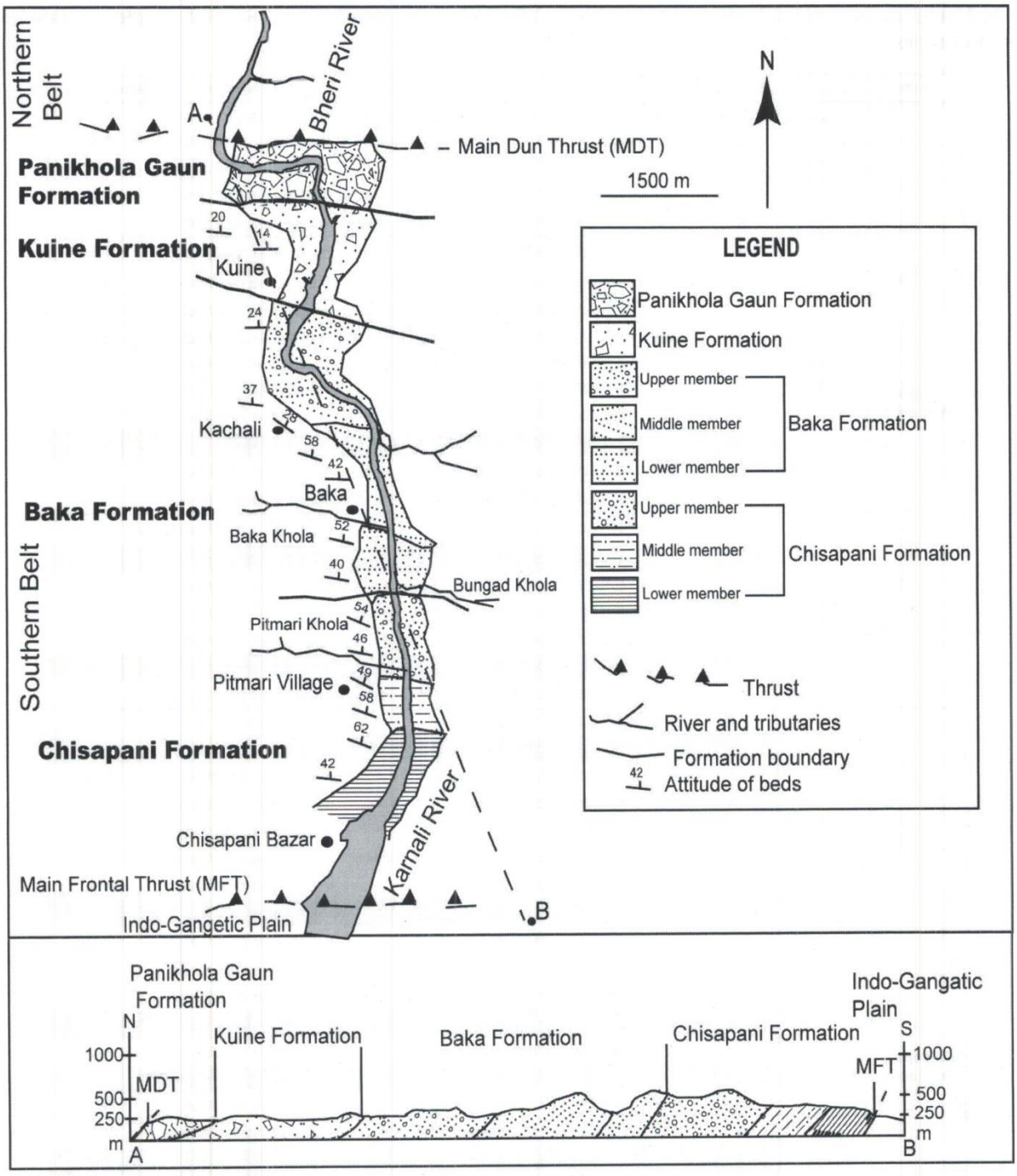

Fig. 2: Geological division of the Siwalik Group along the Karnali River, and geological section along line A-B.

were counted with grid spacing designed to fully cover each slide, at horizontal spacing of 0.2 mm. The detrital modes were recalculated to 100% as the sum of quartz (Q), feldspar (F) and lithic fragments (L) (Table 2). These recalculated parameters were plotted on QFL triangular diagrams for classification (Pettijohn 1975; Folk 1980) and determination of provenance (Dickinson et al. 1983).

Statistical framework

Once all the point counts were completed, compositions were recalculated to 100% for the multivariate statistics, with respect to quartz, feldspar and lithic grains, as well as muscovite, biotite, carbonate and cement. Data were also grouped by formation and grain size /facies (thick- and thin-

Table 1: List of samples with GPS locations, grain size, lithofacies, and bedding type. Shaded samples are thin bedded facies sandstones.

Fmtn	mbr	Sample no	GPS location	Grain size	Lithofacies	Bedding type
Baka Formation	Upper member	G-5	N28°41'59"/ E81°16'30"	coarse (salt & pepper)	trough cross strat., pebbly	thick
		G-3	N28°41'58"/ E81°16'31"	coarse (salt & pepper)	trough cross strat., pebbly	thick
		G-2	N28°41'55"/ E81°16'31"	coarse	trough cross strat., pebbly	thick
		BK-23	N28°41'52"/ E81°16'36"	v. coarse (salt & pepper)	trough cross strat., pebbly	thick
		G-1	N28°41'49"/ E81°16'44"	v. coarse (salt & pepper)	trough cross strat., pebbly	thick
	Middle member	BK-14	N28°41'40"/ E81°16'51"	fine	planar cross stratification	thick
		BK-13	N28°41'33"/ E81°16'51"	coarse (salt & pepper)	trough cross stratification	thick
		F-1	N28°41'31"/ E81°16'51"	coarse (salt & pepper)	trough cross stratification	thick
		E-1	N28°41'31"/ E81°16'51"	coarse (salt & pepper)	trough cross stratification	thick
		D-9	N28°41'25"/ E81°16'50"	coarse (salt & pepper)	trough cross stratification	thick
		D-7	N28°41'10"/ E81°16'56"	fine	planar cross stratification	thick
		BK-11	N28°41'10"/ E81°16'56"	coarse (salt & pepper)	trough cross stratification	thick
		BK-9	N28°41'03"/ E81°16'57"	coarse (salt & pepper)	ripple lamination	thin
		D-6	N28°41'03"/ E81°16'57"	coarse (salt & pepper)	trough cross stratification	thick
		BK-7	N28°40'56"/ E81°17'02"	coarse (salt & pepper)	trough cross stratification	thick
	Lower member	D-5	N28°40'51"/ E81°17'02"	coarse	trough cross stratification	thick
		BK-5	N28°40'49"/ E81°17'03"	fine	massive, concretion	thin
		BK-4	N28°40'45"/ E81°17'03"	coarse (salt & pepper)	trough cross stratification	thick
		D-3	N28°40'43"/ E81°17'03"	coarse (salt & pepper)	trough cross stratification	thick
		D-2	N28°40'36"/ E81°17'04"	coarse (salt & pepper)	trough cross stratification	thick
		BK-2	N28°40'36"/ E81°17'04"	medium	parallel lamination	thin
		D-1	N28°40'33"/ E81°17'05"	medium (salt & pepper)	trough cross stratification	thick
Chisapani Formation	Upper member	C-24	N28°40'21"/ E81°17'02"	medium	parallel lamination	thick
		C-22	N28°40'19"/ E81°17'01"	very fine	parallel lamination	thin
		C-21	N28°40'09"/ E81°17'02"	medium	planar cross stratification	thick
		C-20	N28°40'01"/ E81°17'07"	coarse	planar cross stratification	thick
		B-36	N28°40'01"/ E81°17'07"	coarse	planar cross stratification	thick
		B-35	N28°40'01"/ E81°17'07"	coarse (salt & pepper)	trough cross stratification	thick
		B-17	N28°39'53"/ E81°17'09"	medium	trough cross stratification	thick
		C-15	N28°39'51"/ E81°17'09"	fine	ripple lamination	thin
		B-14	N28°39'51"/ E81°17'09"	coarse	trough cross stratification	thick
		B-8	N28°39'48"/ E81°17'11"	fine	planar cross stratification	thick
		B-6	N28°39'47"/ E81°17'12"	medium	planar cross stratification	thick
		C-12	N28°39'47"/ E81°17'12"	very fine	climbing ripple lamination	thin
		KS-9	N28°39'44"/ E81°17'12"	coarse	trough cross stratification	thick
		KS-8	N28°39'34"/ E81°17'14"	fine	planar cross stratification	thin
		KS-7	N28°39'21"/ E81°17'13"	v. coarse (salt & pepper)	trough cross stratification	thick
	Middle member	KS-6	N28°39'26"/ E81°17'13"	medium	planar cross stratification	thick
		KS-5	N28°39'25"/ E81°17'13"	fine	massive concreted sst	thin
		KS-4	N28°39'21"/ E81°17'14"	fine	planar cross stratification	thin
		C-5	N28°39'21"/ E81°17'14"	fine	ripple lamination	thin
	Lower member	A-39I	N28°39'11"/ E81°17'15"	fine	planar cross stratification	thick
		KS-3	N28°39'11"/ E81°17'15"	fine	trough cross stratification	thick
		KS-2	N28°39'07"/ E81°17'14"	fine	planar cross stratification	thick
		C-3	N28°39'07"/ E81°17'14"	very fine	parallel lamination	thin
		R-1	N28°39'06"/ E81°17'14"	fine	planar cross stratification	thin
		A-3	N28°39'01"/ E81°17'12"	fine	planar cross stratification	thick
		KS-1	N28°39'01"/ E81°17'12"	medium	planar cross stratification	thick

Table 2: Recalculated modal point count data (%) and calculated Q/F and Q/L logratios for the Chisapani and Baka Formations.

Chisapani Formation

	Modal composition (%)												Recalculated QFL			logratio	
Sample	Qtz	Feld	Lithic	Musc	Biot	Chl	CO3	Alt	Mat	Cem	Opq	Oth	Q	F	L	ln Q/F	ln Q/L
C-24	37.2	1.4	14.8	1.4	2.4	0.0	23.8	3.4	7.4	6.6	0.2	1.4	69.7	2.6	27.7	3.3	0.9
C-22	38.0	0.8	25.8	3.8	3.0	0.0	11.0	0.2	7.8	8.6	0.2	0.2	58.8	1.2	39.9	3.9	0.4
C-21	47.2	0.8	34.4	0.4	2.6	0.0	6.0	1.2	2.8	3.4	1.0	0.2	57.3	1.0	41.7	4.1	0.3
C-20	55.4	3.0	14.6	2.2	2.0	0.6	10.8	0.2	4.4	6.2	0.2	0.4	75.9	4.1	20.0	2.9	1.3
B-36	54.8	1.6	13.0	0.4	2.2	0.0	15.8	0.6	7.4	3.6	0.4	0.2	79.0	2.3	18.7	3.5	1.4
B-35	45.2	2.0	15.8	1.0	0.6	0.0	17.4	0.0	8.6	8.8	0.4	0.2	71.7	3.2	25.1	3.1	1.1
B-17	40.8	4.4	37.2	2.6	3.0	0.4	4.4	0.0	2.0	5.2	0.0	0.0	49.5	5.3	45.1	2.2	0.1
C-15	40.0	2.2	20.6	5.0	6.0	0.0	12.8	0.4	5.6	6.0	0.4	1.0	63.7	3.5	32.8	2.9	0.7
B-14	46.8	1.8	20.6	1.8	1.6	0.4	12.4	0.0	5.2	9.4	0.0	0.0	67.6	2.6	29.8	3.3	0.8
B-8	33.0	2.0	21.0	3.2	0.6	0.0	21.8	0.4	5.4	11.0	1.0	0.4	58.9	3.6	37.5	2.8	0.5
B-6	33.0	1.4	19.2	4.0	2.6	0.2	21.0	0.0	8.2	9.8	0.2	0.4	61.6	2.6	35.8	3.2	0.5
C-12	41.0	1.6	16.2	8.2	7.4	0.0	11.8	0.8	4.4	8.2	0.2	0.2	69.7	2.7	27.6	3.2	0.9
KS-9	45.6	2.0	15.6	5.6	4.2	0.0	11.2	0.0	5.6	7.2	0.8	2.2	72.2	3.2	24.7	3.1	1.1
KS-8	37.4	0.8	13.0	3.2	2.0	0.0	20.0	0.6	11.0	11.4	0.2	0.4	73.0	1.6	25.4	3.8	1.1
KS-7	59.8	1.8	22.8	1.8	0.8	0.0	1.2	0.4	4.6	5.6	1.4	0.0	70.9	2.1	27.0	3.5	1.0
KS-6	46.8	4.2	20.6	2.0	1.2	0.4	10.8	0.6	5.4	7.0	0.4	0.6	65.4	5.9	28.8	2.4	0.8
KS-5	45.8	1.8	24.2	1.4	0.2	0.0	7.8	0.0	8.6	9.8	0.4	0.0	63.8	2.5	33.7	3.2	0.6
KS-4	48.8	2.0	19.4	3.0	0.4	0.0	3.8	0.2	9.0	13.0	0.2	0.2	69.5	2.8	27.6	3.2	0.9
C-5	50.6	1.2	29.8	1.4	1.2	0.2	4.6	0.8	5.6	3.8	0.6	0.2	62.0	1.5	36.5	3.7	0.5
A-39I	49.2	2.2	20.2	2.8	2.2	0.0	6.2	0.2	9.0	7.4	0.0	0.6	68.7	3.1	28.2	3.1	0.9
KS-3	51.2	2.2	15.2	3.4	2.4	0.1	11.0	0.6	5.4	7.0	1.2	0.4	74.6	3.2	22.2	3.1	1.2
KS-2	56.0	1.6	22.2	1.2	0.6	0.6	3.6	1.6	3.4	8.2	0.0	1.0	70.2	2.0	27.8	3.6	0.9
C-3	36.4	1.0	4.8	3.0	0.2	0.0	10.4	0.0	8.0	35.0	0.6	0.6	86.3	2.4	11.4	3.6	2.0
R-1	36.0	1.2	22.2	0.4	0.4	0.2	17.0	0.4	10.2	12.0	0.6	0.6	60.6	2.0	37.4	3.4	0.5
A-3	54.6	1.0	19.6	1.2	0.6	0.0	7.2	0.0	6.0	9.2	0.2	0.4	72.6	1.3	26.1	4.0	1.0
KS-1	55.4	4.0	18.4	1.0	0.4	1.0	5.6	1.6	3.8	7.4	0.2	1.2	71.2	5.1	23.7	2.6	1.1
Mean	***45.6***	***1.9***	***20.0***	***2.5***	***2.0***	***0.2***	***11.1***	***0.5***	***6.3***	***8.9***	***0.4***	***0.5***	***67.9***	***2.8***	***29.3***	***3.2***	***0.8***
Max	*59.8*	*4.4*	*37.2*	*8.2*	*7.4*	*1.0*	*23.8*	*3.4*	*11.0*	*35.0*	*1.4*	*2.2*	*86.3*	*5.9*	*45.1*	*2.7*	*0.6*
Min	*33.0*	*0.8*	*4.8*	*0.4*	*0.2*	*0.0*	*1.2*	*0.0*	*2.0*	*3.4*	*0.0*	*0.0*	*49.5*	*1.0*	*11.4*	*3.9*	*1.5*
S.D	*7.8*	*1.0*	*6.7*	*1.8*	*1.8*	*0.3*	*6.2*	*0.7*	*2.3*	*5.9*	*0.4*	*0.5*	*7.7*	*1.2*	*7.6*	*1.8*	*0.0*

Baka Formation

	Modal composition (%)												Recalculated QFL			logratio	
Sample	Qtz	Feld	Lithic	Musc	Biot	Chl	CO3	Alt	Mat	Cem	Opq	Oth	Q	F	L	ln Q/F	ln Q/L
G-5	41.0	4.2	21.8	4.4	1.8	0.2	14.6	0.0	4.4	7.2	0.0	0.4	61.2	6.3	32.5	2.3	0.6
G-3	40.0	3.2	20.6	4.6	3.0	0.2	12.0	0.0	9.0	6.6	0.2	0.6	62.7	5.0	32.3	2.5	0.7
G-2	39.8	3.4	20.2	2.4	6.6	0.4	12.4	0.0	7.2	7.4	0.0	0.2	62.8	5.4	31.9	2.5	0.7
BK-23	37.0	1.0	19.8	6.0	12.2	0.2	8.8	1.0	5.6	7.2	0.2	1.0	64.0	1.7	34.3	3.6	0.6
G-1	46.0	3.8	19.8	4.8	3.4	0.2	6.8	2.0	4.6	8.4	0.0	0.2	66.1	5.5	28.5	2.5	0.8
BK-14	49.0	2.8	16.4	2.2	5.4	0.4	7.2	1.8	7.6	6.4	0.2	0.6	71.9	4.1	24.1	2.9	1.1
BK-13	47.0	2.0	14.2	4.8	10.8	3.4	3.2	1.4	3.8	8.4	0.2	0.8	74.4	3.2	22.5	3.2	1.2
F-1	41.8	5.0	25.8	4.2	2.6	0.4	12.0	0.0	3.6	4.4	0.0	0.2	57.6	6.9	35.5	2.1	0.5
E-1	36.8	6.2	16.0	3.2	5.2	0.4	21.8	0.0	4.4	5.2	0.0	0.8	62.4	10.5	27.1	1.8	0.8
D-9	42.6	3.6	25.4	6.2	4.6	0.0	5.2	0.8	3.4	7.6	0.0	0.6	59.5	5.0	35.5	2.5	0.5
D-7	41.8	6.2	15.8	0.6	5.8	1.6	17.0	0.0	5.2	6.0	0.0	0.0	65.5	9.7	24.8	1.9	1.0
BK-11	41.8	2.2	17.0	5.6	6.0	1.6	11.0	1.2	7.0	6.4	0.2	0.0	68.5	3.6	27.9	2.9	0.9
BK-9	23.4	0.2	4.4	12.0	16.2	1.8	22.2	0.4	6.2	12.6	0.2	0.4	83.6	0.7	15.7	4.8	1.7
D-6	48.6	4.6	22.0	1.4	2.2	0.0	10.4	0.0	6.0	4.6	0.2	0.0	64.6	6.1	29.3	2.4	0.8
BK-7	60.0	2.2	12.6	0.6	2.2	0.0	8.6	0.6	8.2	4.2	0.0	0.8	80.2	2.9	16.8	3.3	1.6
D-5	42.6	5.6	15.8	0.6	1.4	0.2	17.4	0.0	6.8	8.8	0.4	0.0	66.6	8.8	24.7	2.0	1.0
BK-5	28.2	1.0	6.6	3.6	5.8	0.0	25.2	1.4	14.8	12.4	0.0	1.0	78.8	2.8	18.4	3.3	1.5
BK-4	52.0	5.0	16.4	2.6	1.2	0.0	11.2	0.4	6.6	4.6	0.0	0.0	70.8	6.8	22.3	2.3	1.2
D-3	56.2	3.8	16.6	3.0	2.6	0.4	6.6	0.0	5.0	5.0	0.2	0.6	73.4	5.0	21.7	2.7	1.2
D-2	43.0	4.4	18.6	3.8	3.2	0.0	11.8	0.0	5.4	8.8	0.4	0.8	65.2	6.7	28.2	2.3	0.8
BK-2	41.8	1.2	14.8	13.2	9.8	0.6	11.4	0.4	2.6	4.6	0.0	0.4	72.3	2.1	25.6	3.6	1.0
D-1	50.0	2.2	20.2	1.2	2.4	0.2	12.4	0.0	4.8	6.2	0.2	0.2	69.1	3.0	27.9	3.1	0.9
Mean	***43.2***	***3.4***	***17.3***	***4.1***	***5.2***	***0.6***	***12.2***	***0.5***	***6.0***	***7.0***	***0.1***	***0.4***	***68.2***	***5.1***	***26.7***	***2.7***	***1.0***
Max	*60.0*	*6.2*	*25.8*	*13.2*	*16.2*	*3.4*	*25.2*	*2.0*	*14.8*	*12.6*	*0.4*	*1.0*	*83.6*	*10.5*	*35.5*	*4.8*	*1.7*
Min	*23.4*	*0.2*	*4.4*	*0.6*	*1.2*	*0.0*	*3.2*	*0.0*	*2.6*	*4.2*	*0.0*	*0.0*	*57.6*	*0.7*	*15.7*	*1.8*	*0.5*
S.D	*8.1*	*1.7*	*5.1*	*3.2*	*3.9*	*0.8*	*5.6*	*0.7*	*2.6*	*2.3*	*0.1*	*0.3*	*6.8*	*2.5*	*5.7*	*0.7*	*0.3*

bedded sandstones) to analyze other factors affecting the composition of the sediments (Table 1).

Univariate statistics (arithmetic mean and standard deviation) are widely used in provenance analysis (Ingersoll 1978; Howard 1994). However, both parameters are semi-quantitative, because they assume a normal distribution of each component and independence of the components from each other (Allen and Johnson 2010). These assumptions are not valid in ternary diagrams (Weltje 2002). Recent work by Weltje (2002), Ohta and Arai (2007) and Ingersoll and Eastmond (2007) used several multivariate statistical methods to evaluate sandstone compositions. These methods included Principal Component Analysis (PCA), multivariate means, and confidence regions.

PCA is a technique that combines numerous variables into several independent latent variables that underline the multivariate data. PCA can be viewed as a search for the orthogonal coordinates that explain the greatest amount of variation within the data. In undertaking the PCA and expressing the results graphically on ternary diagrams, we followed the approaches described by Weltje (2002), Von Eynatten et al. (2003), and Buccianti and Esposito (2004). These methods are based on the statistical analytical technique for compositional data described by Aitchison (1986). In brief the following sequence of operations was carried out, using CoDaPack 2 software (Thio-Henestrosa and Comas 2011).

1. The petrographic compositional data, whose natural sample space is a simplex, were mapped into Euclidean real sample space using log-ratio transformation (e.g., clr, alr).
2. Following the log-ratio transformation, the first and second principal components were extracted in the usual way via PCA, using biplots.
3. The log-ratio coordinates were back-transformed to the two-dimensional simplex space ternary diagrams by inverse log-ratio transformation.
4. Within the ternary diagrams, we utilized Weltje's multivariate means and 90%, 95%, and 99% confidence ellipsoids. The boundaries of the multivariate confidence regions for population means were calculated to discriminate the factors controlling the compositions of the sediments.

RESULTS

Petrography of the individual formations

Chisapani Formation

Of the 26 samples analyzed for the Chisapani Formation, seven were taken from the lower member, four from the middle member, and 15 from the upper member (Tables 1 and 2). The Chisapani Formation sandstones are matrix-poor, moderately to well-sorted, and individual grains are sub-rounded to rounded. Quartz grains are mainly monocrystalline, but some polycrystalline grains are present (Fig. 3 A, B). Quartz is the dominant mineral in this formation, ranging from 33% (B-6) to 59.8% (KS-7). Feldspar contents are low, ranging from only 0.8% to 4.0% (KS-1). The feldspars are mainly plagioclase and orthoclase (Fig. 3C). Average feldspar content is approximately equal in all three members. Lithic grain contents vary widely, from 4.8% (C-3) to 37.2% (B-17) (Table 2). The lithic grains are mainly sedimentary and metamorphic, although some plutonic clasts also occur. In all three members the metamorphic lithics are dominantly quartz-mica schists and phyllites. Muscovite and biotite (mica) occur as accessory minerals in the Chisapani Formation. The amount of mica present ranges from 0.4% to 8.2% for muscovite, and 0.2% to 7.4% for biotite. The percentage of mica increases toward the upper member. Carbonate is other important constituent in the Chisapani Formation, occurring as intraclasts, and cement (Fig. 3A, C). Carbonate contents range from 1.2% (KS-7) to 23.8% (C-24), and increase toward the upper member. Mica and carbonates are the only components to show noticeable stratigraphic change at some intervals within this formation (Table 2).

Baka Formation

The Baka Formation is represented by 22 sandstones, with seven from the lower member, ten from the middle member, and five from the upper member (Tables 1 and 2). The sandstones are matrix-poor and are moderately to well sorted, and contain angular to sub-rounded framework grains. Quartz is again the dominant mineral, with contents ranging from 23.4% (BK-9) to 60.0% (BK-7). Feldspar grains consist of plagioclase, orthoclase and microcline, and form up to 6.2% of the mode (D-7, E-1). Lithics are mainly metamorphic rock fragments such as mica schists, foliated quartz, and phyllite (Fig. 3D, 3E and 3F). The proportions of biotite and muscovite range from 1.2% (BK-4) to 6.2% (BK-9) and 0.6 % (BK-7) to 12% (BK-9) respectively, and contents increase toward the upper member (Table 3), reaching maximums of 12.2% (biotite) and 6.0% (muscovite) in sample BK-23 (Table 2, Fig. 3F). Carbonate contents contain range from 3.2% (BK-13) to 25.2% (BK-5), but no clear stratigraphic change is evident. Heavy minerals, opaque minerals and chlorite occur in minor amounts (Table 2). Feldspar and Mica contents show the same changes in some intervals in this formation.

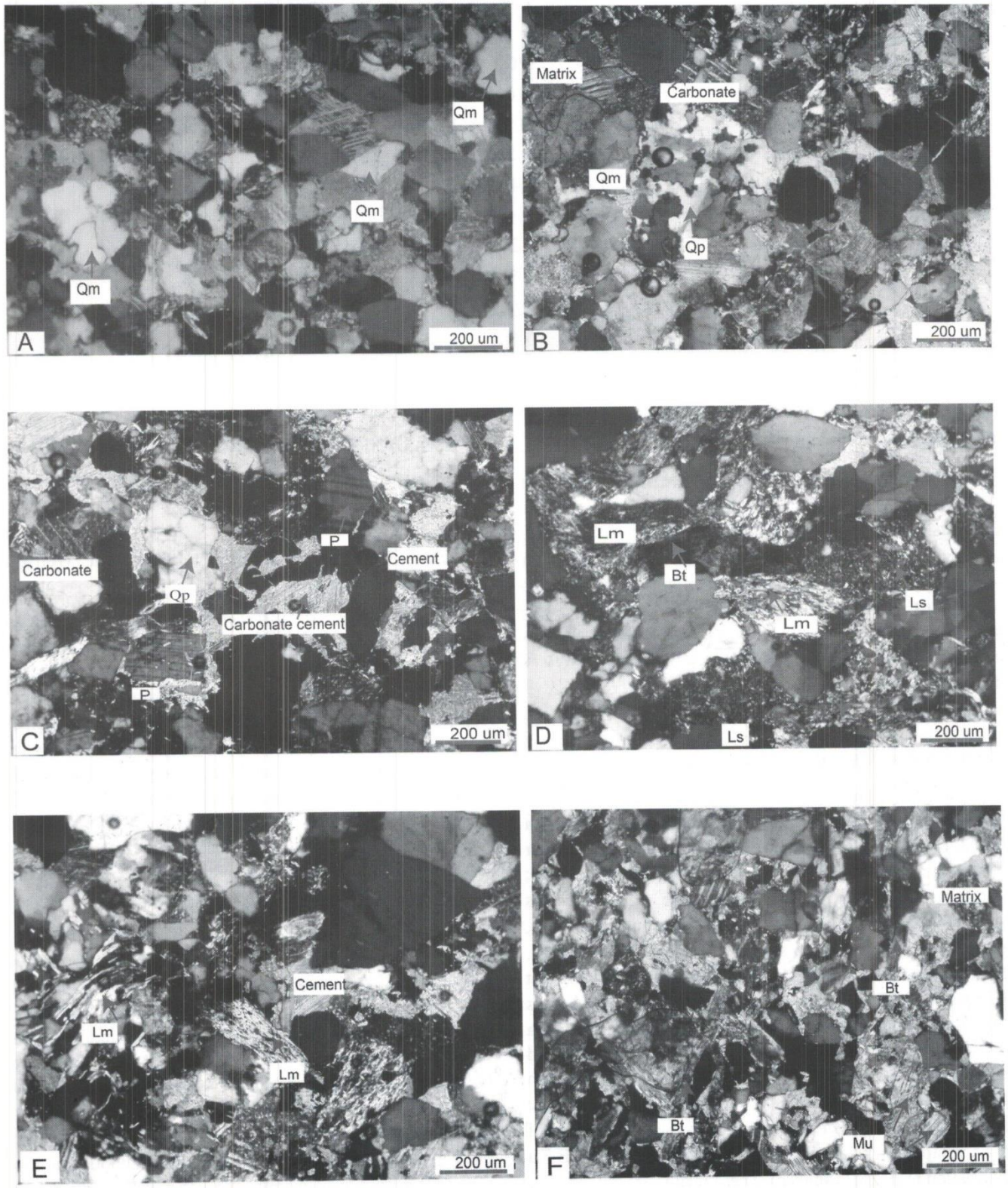

Fig. 3: Photomicrographs of sandstones from the Chisapani and Baka Formations. (A) Monocrystalline quartz (Qm). (B) Polycrystalline quartz (Qp). (C) Plagioclase feldspar and carbonates. (D) Sedimentary (Ls) and metamorphic lithic grains (Lm). (E) Metamorphic lithic grains (Quartz-mica schist). (F) Mica grains, variegated colour indicates muscovite (Mu) and dark brown colour indicates biotite (Bt).

Table 3: Results of Principal Component Analysis (PCA) for the Chisapani and Baka Formations.

	PC1	PC2	PC3	PC4	PC5	PC6
Quartz	0.247	-0.055	0.067	-0.364	0.188	-0.788
Feldspar	0.369	-0.500	0.156	0.630	0.198	0.101
Lithics	0.282	-0.207	0.171	-0.482	-0.569	0.386
Muscovite	-0.415	0.406	0.586	0.298	-0.267	-0.129
Biotite	-0.716	-0.440	-0.220	-0.192	0.228	0.112
Carbonate	0.045	0.281	-0.741	0.285	-0.365	-0.107
Cement	0.188	0.516	-0.018	-0.175	0.588	0.424
Varience explained (%)	45.76	22.62	17.27	8.92	3.96	1.47
Cum. Prop. Exp.	0.458	0.684	0.857	0.946	0.985	1.000

Classification of the sandstones

According to this classification scheme of Pettijohn (1975), most samples are lithic arenites, and the remainder sub-litharenites (Fig. 4 A). Using the Folk (1980) diagram, slightly higher feldspar content in a few Baka Formation sandstones leads to their classification as feldspathic litharenites, while the majorities are litharenites (Fig. 4B). However, there is no significant contrast in the compositions of these two formations, and high quartz/feldspar ratio is maintained throughout the succession.

Comparison with the other Siwalik sections

The QFL characteristics of the Karnali River samples were also compared with those from other Siwalik sections in the Surai Khola, Arung-Tinau Khola, Hetauda, and Muskar Khola districts (Dhital et al. 1995; Tokuoka et al. 1986; Tamrakar et al. 2003; Chirouze et al. 2012) (Fig. 4C). This shows that QFL compositions are similar among these areas, except for lower feldspar content in the Karnali section. Surai Khola and Arung Khola sandstones have the highest feldspar and lithic fragment contents, and are classified as litharenites and feldspathic litharenites. Similarly, Hetauda section sandstones have indicates that higher feldspar and quartz contents, and are classified as lithic arenites through to arkosic arenites. The Muskar Khola samples contain the least feldspar. The overall recalculated QFL composition of the Chisapani Formation is $Q_{68}F_3L_{29}$, and that of the Baka Formation $Q_{68}F_5L_{27}$ (Tables 2). These results are comparable with previous studies from the Surai Khola and Bakiya Khola sections, which are characterized by quartzolithic compositions of $Q_{57}F_4L_{39}$ and $Q_{59}F_6L_{35}$, respectively (Critelli and Ingersoll 1994).

ANALYSIS OF CONTROLLING FACTORS USING MULTIVARIATE STATISTICS

Principal Component Analysis (PCA) and Weltje's confidence regions

PCA loadings of clr-transformed data are presented in Table 3. The first principal component (PC1) shows a positive correlation with clr-transformed quartz, feldspar, lithics, carbonate and cement components, and negative correlation with muscovite and biotite. The second principal component (PC2) is positively correlated with muscovite, carbonates and cements, and negatively correlated with quartz, feldspar, and lithics components. PC1 and PC2 capture 46% and 24% of the total variability, respectively. Collectively 70% of the total variability is explained by these two components, with a smaller amount (17%) being accounted for the third principal component (PC3).

PC1 and PC2 are illustrated as a biplot (Gabriel 1971; Aitchison and Greenacre 2002) in Fig. 5. Samples from the Chisapani Formation plot randomly on the biplot. PC1 is positively correlated with quartz, feldspar, and lithic fragments. Carbonate is also positively correlated, but plots in a near-perpendicular direction to PC1. Muscovite and biotite are negatively correlated in PC1. Similarly, carbonate muscovite and cement are positively correlated in PC2, with all other components negatively correlated. Samples from the Baka Formation also plot randomly, although a few samples tend to be concentrated near the quartz and feldspar components. The carbonate is mainly originated from the Lesser Himalayan sources and feldspar, muscovite and biotite are indicators of the Higher Himalayan source. These components of data suggest that PC1 probably related to the

mixed sources from the Lesser and Higher Himalayas, and PC2 is correlated with the Higher Himalaya (Fig. 5). The data for both formations are strongly influenced by both PC1 and PC2, probably due to mixed sediments from the Lesser and Higher Himalayas.

The PCA biplot confirms that there is a strong relationship between quartz, feldspar and lithic grains in both the Chisapani and Baka Formations (Fig. 5). To more clearly discriminate between these components, we have used another multivariate statistical method adopted by Weltje

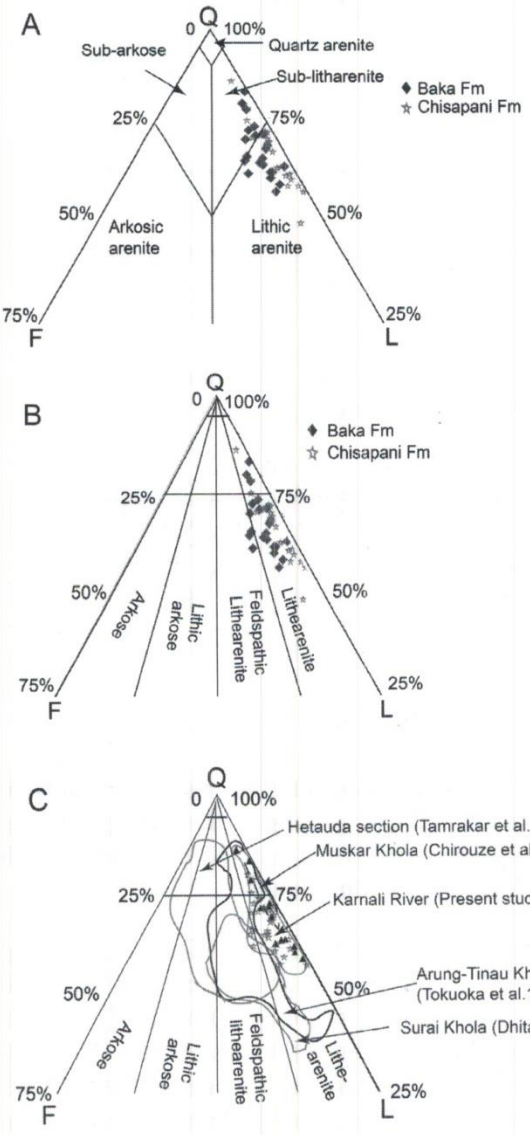

Fig. 4: Classification of Karnali River Siwalik sandstones . (A) QFL diagram based on Pettijohn (1975), showing sublitharenite to lithic arenite sandstones. (B) QFL diagram of Folk (1980) showing litharenite to feldspathic litharenite sandstones. (C) Comparison with sandstones from different sections of the Siwalik Group, Nepal.

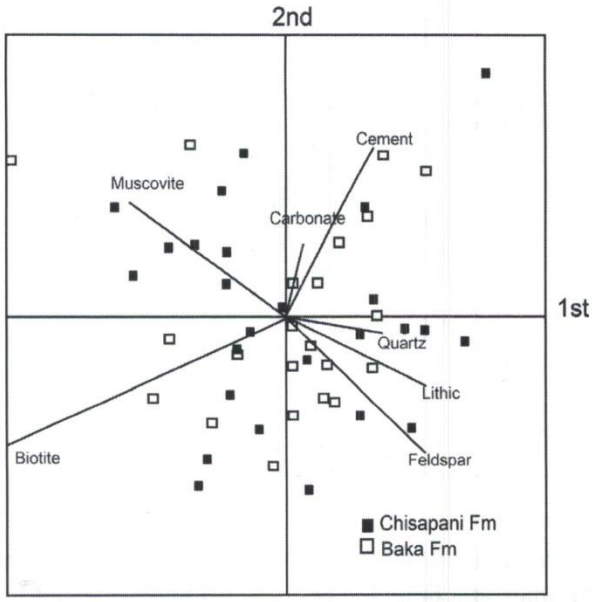

Fig. 5: Principal Component Analysis (PCA) biplot of the clr-transformed data from Table 2. Scattered data indicates little variation in sediment composition between the fomations (see text for details).

(2002). This method is formalized by use of the multivariate additive logistics normal distribution (Aitchison 1986). Stattegger and Mortan (1992), Prins and Weltje (1999) and Garzanti et al. (2000) have also used ternary confidence regions for petrographic data, based on this model. The purpose of these confidence regions were given by Weltje (2002) as:

1. Confidence regions of the entire population can be used to predict the range of variation in observations;

2. Confidence regions of the population mean are useful for deciding if samples differ significantly from each other.

The multivariate confidence regions of the Chisapani and Baka Formations are shown in Figure 6. Most of the data falls within the 90% confidence regions of both formations. The mutual clustering of the Chisapani and Baka Formations data and the nearly total overlap of their confidence regions indicates general lack of significant compositional variation between the formations, and that the sediments mixed (Weltje 2002). This suggests the sediments in each formation were simultaneously derived from both the lesser Himalaya and Higher Himalaya. Slight change in the composition of the Baka Formation and subtle shift of the data towards the 95% and 99% confidence regions likely reflects some contribution from a different source area (i.e., Higher Himalaya), or some local influence such as hydraulic sorting during transportation (Weltje 2002; Allen and Johnson 2010) (Fig. 6B).

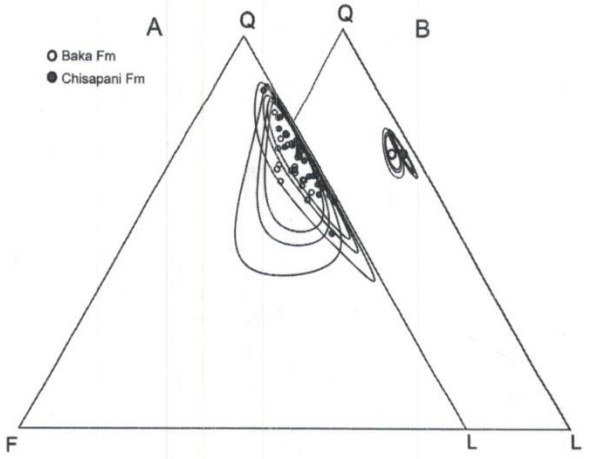

Fig. 6: Multivariate ellipsoids (Weltje 2002) for the Chisapani and Baka Formations. Confidence regions are 90%, 95% and 99%. (A) Predictive regions of the data points. (B) Confidence regions of the population mean. See text for details.

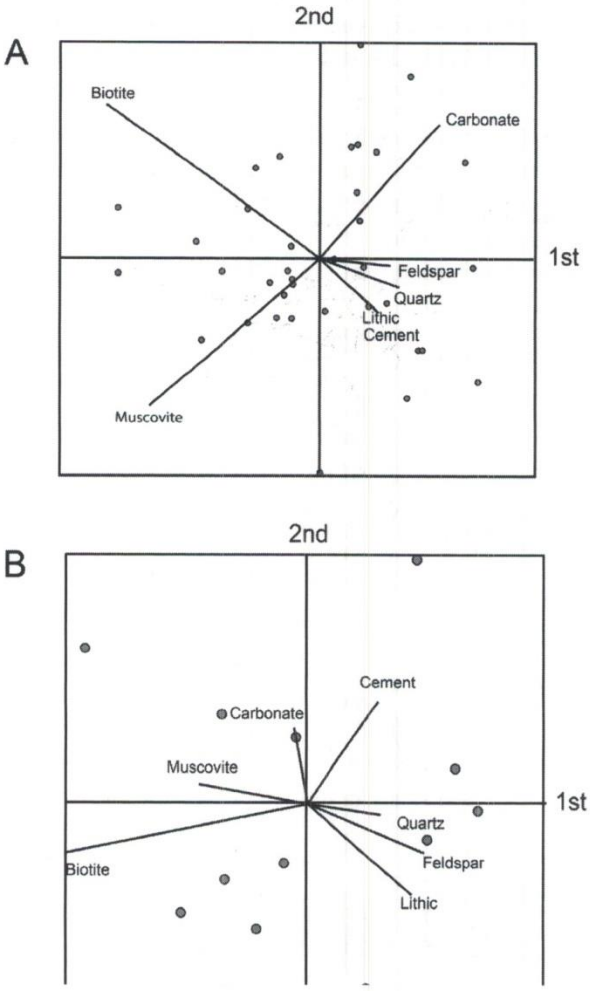

Fig. 7: Principal Component Analysis (PCA) biplot of clr-transformed data by grain size. Data are grouped on the basis of facies and grain size. (A) thick-bedded; (B) thinly-bedded. See text for details.

Grain size and facies control on sediments (thick vs. thin-bedded sandstones)

Thick-bedded sandstones in the Karnali section consist mainly of trough to planar cross-stratified, medium to coarse-grained sandstones, with bed thicknesses ranging from 4.0 to 10.0 m. These thick-bedded sandstones are interpreted as channel deposits. The thin-bedded (shaded part) sandstones sampled here are mainly very fine to medium-grained, and cross-stratified to rippled (Table 1). Bed thicknesses range from 0.5 to 2.0 m, and the beds are interpreted as being either flood plain or crevasse splay deposits (Sigdel et al. 2011).

We have also applied the multivariate statistics method here to test for contrast between grain size/facies groups, based on the compositions of the thinly and thickly bedded sandstones (Table 1). The biplot from the PCA analysis shows random distribution in all coordinate planes (Fig. 7). The Weltje triangular confidence 90%, 95% and 99% regions for the two facies also overlap each other, indicating the sediments are well mixed, and no specific control is exercised by the principal components (Fig. 8). The slightly different locations of the population means of the confidence regions suggest changes in the source area, or minor influence by the facies/grain size of the sediments.

Climatic-physiographic control on sediments

A general petrographic measure of the weathering trends of sandstone may be defined in term of the log-ratios of principal framework elements (cf Aitchison 1986), for example as log (Q/F) or log (Q/L), where Q = quartz, F = feldspar and L = lithic fragments (Weltje 1994). The log-ratios for individual samples are listed in Tables 2. For many types of sand, values of both log-ratios are expected to correlate with weathering intensity, because quartz is more resistant to weathering than feldspar and lithic fragments. The combination of these log-ratios in a single diagram permits the distinction of parent rock type, weathering history, and paleotopography (Weltje et al. 1998) (Fig. 9). Based on this diagram, all except two of the Karnali samples fall in the field of weathering index 1 (Fig. 9). The

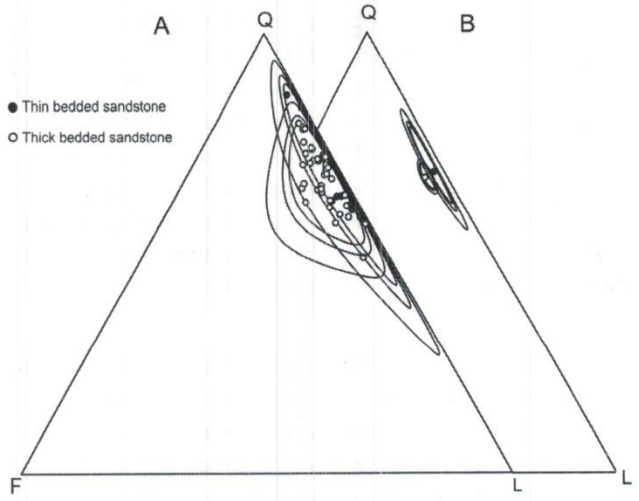

Fig. 8: Multivariate ellipsoids (Weltje 2002) of the thick and thinly-bedded sandstones Confidence regions are 90%, 95% and 99%. (A) Predictive regions of the data points. (B) Confidence regions of the population mean. See text for details.

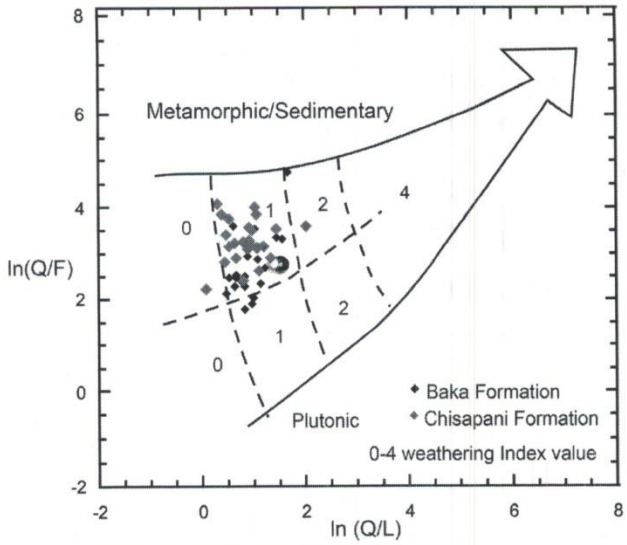

Semi quantitaive weathering Index		High Mountain 0	Moderate Hill 1	Low plain 2
Climate: (Semi) arid and mediterranean	0	0	0	0
Temparate subhumid	1	0	1	2
Tropical humid	2	0	2	4

Fig. 9: Log-ratio plot after Weltje (1994). Q-quartz; F-Feldspar; L-lithic fragments. Fields 0-4 refer to the semi-quantitative weathering indices defined on the basis of relief and climate, as indicated in the table.

Chisapani Formation samples mainly fall near the boundary between weathering index 0 and 1, towards metamorphic and sedimentary parentage. Samples from the Baka Formation plot nearer the boundary between metamorphic/ sedimentary and plutonic parentage. These indices indicate that the sediments were mainly derived from high mountains (Higher Himalaya) and moderate hills (Lesser Himalaya), and the influence of climate on the sediment compositions was very small (0-1) (Fig. 9).

DISCUSSION

The multivariate statistical analysis (PCA biplots and Weltje's confidence interval of geometric means and ellipsoids) enables direct comparison between the datasets to evaluate if minute differences in composition can be detected. These analyses found slight variation in sediment composition between the Chisapani and Baka Formations. These contrasts are mainly linked to the source area and tectonics, rather than being controlled by the facies, grain size, or climate.

Regional controlling factors (source lithology and tectonic setting)

All Karnali Siwalik sandstones fall well within the recycled orogen provenance field on the QFL provenance diagram of Dickinson et al. (1983), indicating that bulk compositions do not vary significantly within the section (Fig. 10A). The sandstones are characteristically rich in quartz and lithic grains, and poor in feldspar. Within such recycled orogens, clastic detritus is dominantly derived from sedimentary and metamorphic rocks exposed and eroded by orogenic uplift of fold belts and thrust sheets (Dickinson and Suczek 1979; Dickinson 1985).

The sandstones of the Karnali River section are characterized by an assemblage of monocrystalline and polycrystalline quartz, feldspar, carbonates, mica schist lithics, muscovite and biotite. These detrital grains were derived mainly from sedimentary and low- to high-grade metamorphic sources. The abundant monocrystalline quartz grains are of plutonic origin (Young 1976), probably from the Dadeldhura granite (Szulc et al. 2006; Bernet et al. 2006).

Temporal changes in petrographic modes in the Karnali section indicate that the proportion of carbonates increased after 13.0 Ma (Fig. 11). These were probably derived from

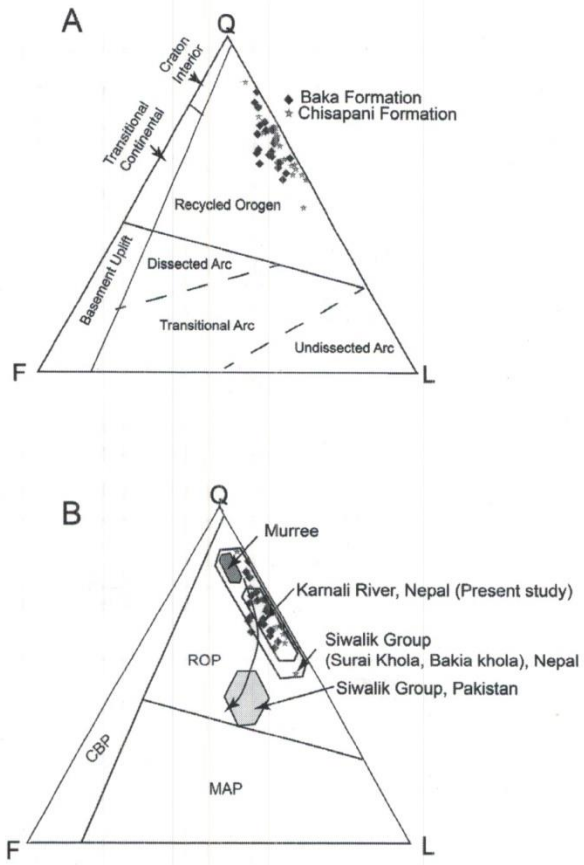

Fig. 10: QFL provenance plot (Dickinson, et al. 1983) for the Karnali sandstones. A) QFL plot for the Siwalik Group along the Karnali River section, indicating derivation from a recycled orogen source. B) QFL plot showing regional comparison in the Himalaya foreland basin (modified from Critelli and Ingersoll 1994).

the Lesser Himalaya. This result is consistent with an increase in $^{87}Sr/^{86}Sr$ ratio from 12.0 Ma onwards (Szulc et al. 2006). Huyghe et al. (2001, 2005) also reported more negative εNd isotopes values from the Karnali section after 13.0 with peak around 10.0 Ma (Fig. 11). Similarly, the proportions of feldspar and mica grains (Higher Himalayan source) decrease in the interval from 12.0-9.0 Ma. The combination of these results suggests that between 12.0-9.0 Ma the Karnali Siwalik sediments were mainly derived from the Lesser Himalayan zone, probably due to the development of the Lesser Himalayan duplex. Similarly, DeCelles et al. (1998) and Robinson et al. (2001) documented strongly negative εNd isotopes values from other Siwalik sections (Khutia Khola, Surai Khola) at about 12.0-9.0 Ma, indicating Lesser Himalayan origin. The slight increase in modal feldspar and mica observed from 9.5 to 6.0 Ma hints at an increasing contribution from the Higher Himalaya, perhaps reflecting deeper erosion of both granitoids and high-grade metamorphic rocks in that unit. This result is also consistent with increased proportions of heavy minerals (Szulc et al. 2006) and the shift to positive εNd isotope values (Huyghe et al. 2001, 2005) in that interval (Fig. 11). Decrease in feldspar and mica content after 6.0 Ma, together with somewhat higher carbonate content, indicates increased supply of the Lesser Himalayan-derived sediments, as also supported by shift to more negative εNd isotopes values (Huyghe et al. 2001, 2005). However, heavy mineral assemblages (Szulc et al. 2006) and significant mica contents indicate that sediments also continued to be supplied from the Higher Himalaya after 6.0 Ma (Fig. 11).

By combining our petrographic results with previous isotopic and age data, we can constrain provenance of the Karnali River Siwalik succession. Our data confirms that the sediments were mainly derived from the Higher Himalaya and Lesser Himalaya, throughout the period of deposition. The Higher Himalaya was a major source terrain even in the early stage (16.0 Ma) of deposition of the Siwalik Group, with increased sediment supply from the Lesser Himalaya after 13.0 Ma, concurrent with continued supply from the Higher Himalaya. It seems that the Higher Himalaya has maintained a high elevation at least since the Miocene, and that the Lesser Himalaya may have undergone uplift (Lesser Himalayan Duplex) after 13.0 Ma, as shown by the petrographic analysis in this study. However, appearance of 'salt and pepper' sandstones (increase in feldspar and mica grains) in the Middle Siwalik after 9.6 Ma indicates dominant supply from the Higher Himalayan source. This is comparable with results from the Surai Khola, Tinau Khola and Bakia Khola sections, albeit with some time variation (8.5 to 9.5 Ma). Our petrographic results together with mica age (Szulc et al. 2006) and fission track (Bernet et al. 2006) data from all Siwalik sections suggest lateral continuity in tectonic uplift of the Himalaya, but an earlier beginning in far western Nepal.

Comparison with the surrounding area

Based on the QFL scheme of Dickinson et al. (1983), Karnali River sandstones plot in the recycled orogen field, consistent with previous results from the Surai Khola and Bakiya Khola sections (Critelli and Ingersoll 1994). The Arung-Tinau Khola and Hetauda-Bakia Khola sections have the highest feldspar and lithic grain contents among all Siwalik sections, and their sandstones are classified as litharenites and feldspathic arenites. These compositional variations are probably due to contributions from Lesser Himalayan granitoids such as the Agra Granite and the Palung Granite in west-central and eastern Nepal. The recycled orogen provenance of the Karnali samples is also consistent with that for Siwalik sandstones from the Potwar Plateau (Fig. 10B). The only significant different is the

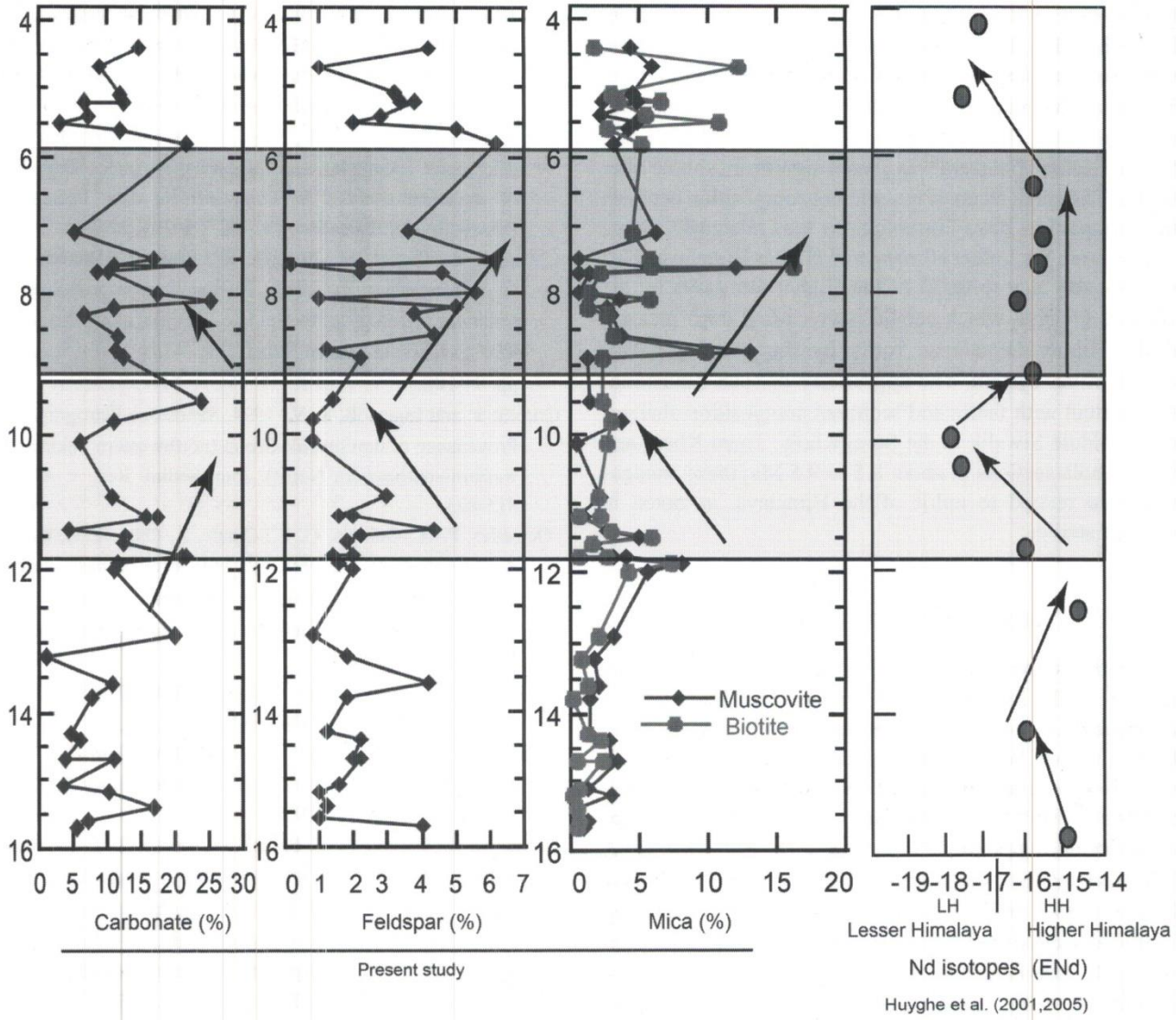

Fig. 11: Vertical variations of carbonate, feldspar, and mica content in Karnali River sandstones with depositional age, and comparison with εNd isotopes values from Huyghe et al. (2001; 2005).

higher feldspar content in the Potwar Plateau relative to the Siwalik Group in Nepal. This compositional variation in the Potwar Siwalik sediments may be related to contributions of detritus derived from volcanic sources in their hinterland (Critelli and Ingersoll 1994).

CONCLUSIONS

Sandstone petrography of the Siwalik Group along the Karnali River shows that the framework grains are mainly quartz (Q), feldspars (F) and rock fragments (L; mainly sedimentary and metamorphic rocks) as major constituents, with mica, chlorites, opaques, and altered minerals occurring as minor accessories. QFL diagrams indicate the Karnali sandstones are classified as sub-litharenites to litharenites with recycled orogen provenance, consistent with previous petrographic analysis of Siwalik sandstones in the Surai Khola, Bakiya Khola, and Potwar Plateau.

Multivariate statistics analysis shows that the sediments are well-mixed. Slight variations in sediment composition between the Chisapani and Baka Formations are mainly linked to the differing source areas and tectonics, rather than to facies, grain size, and climate. Observed changes in the detrital modes (feldspar, lithic grains, mica, and carbonates) suggest that the sources of Karnali sandstones were primarily sedimentary and metamorphic rock terrains.

The detrital modes together with previous isotopic and age data suggest that most of the detritus was derived from the Higher Himalaya, even at an early stage of deposition, with simultaneous contribution from the Lesser Himalaya. However, the distinctive 'salt and pepper' sandstones observed in the Baka Formation (Middle Siwalik) indicate that the Higher Himalaya was a more significant source after 9.6 Ma. The small changes in sediment composition between the Chisapani to Baka Formations is thus related to source change, from the Lesser Himalaya to Higher Himalaya. This was probably due to uplift of the Higher Himalaya by the collision process, which should have caused deep incision of the Higher Himalayan rocks by the existing paleo-Karnali River system. The appearance of such sandstones is consistent with facies and sediment composition changes in the Middle Siwalik in the Surai Khola, Tinau Khola and Bakia Khola sections at about 8.5 to 9.5 Ma; these changes were also related to uplift of the Himalaya, as noted in previous studies.

ACKNOWLEDGEMENTS

We thank the ministry of Education, Culture, Sports, Science and Technology of Japan for providing a Monbukagakusho (MEXT) scholarship for Ph.D. study to the first author. We also thank to Dr. B.P Roser for critical reading and helpful comments on early version of manuscript, to Emeritus Prof. Dr. Y. Sawada of Shimane University for his advice during point-counting and to Dr. P.D. Ulak, Dr. A P. Gajurel for their valuable suggestions during fieldwork. Special thanks to K. N. Pokharel, S. Dhakal for helping in official works to export samples and Biraj Gautam, Dr. Basanta R. Adhikari, Prabhat C. Neupane, Trilok C. Bhatta, Hitendra R. Joshi, Lalit Rai, and Ajit Sapkota for their assistance during fieldwork.

REFERENCES

Aitchison, J., 1986, The Statistical Analysis of Compositional Data. Chapman & Hall, London, 416 p.

Aitchison, J. and Greenacre, M., 2002, Biplots of compositional data. Jour. Roy Stat. Soc., Ser. C, Appl. Stat, v. 51, pp. 375–392.

Allen, J. L. and Johnson C. L, 2010, Facies control on sandstone composition (and influence of statistical methods on interpretations) in the John Henry Member, Straight Cliffs Formation, Southern Utah, USA. Sedim. Geol., v. 230, pp. 60-75.

Amatya, K. M. and Jnawali, B. M., 1994, Geological map of Nepal (Scale 1:1000, 000). Department of Mines and Geology (DMG), Kathmandu, Nepal.

Bernet, M., Van Der Beek, P., Pik, R., Huyghe, P., Mugnier, J-L., Labrin, E. and Szulc, A. G., 2006, Miocene to recent exhumation of central Himalaya determine from combined detrital zircon fission-track and U/Pb analysis of Siwalik sediments, western Nepal. Basin Res., v. 18, pp. 393-412.

Buccianti, A. and Esposito, P., 2004, Insights into Late Quaternary calcareous nannoplankton assemblages under the theory of statistical analysis for compositional data. Palaeogeogr. Palaeoclimatol. Palaeoecol, v. 202, pp. 209–227.

Chirouze, F., Bernet, M., Huyghe, P., Erens V., Dupont-Nivet, G. and Senebier, F., 2012, Detrital thermochronology and sediment petrology of the middle Siwaliks along the Muksar Khola section in eastern Nepal. Jour. Asian Earth. Sci., v. 44, pp. 94-106.

Critelli, S. and Ingersoll, R. V., 1994, Sandstone Petrography and Provenance of the Siwalik Group (northwestern Pakistan and western-southeastern Nepal). Jour. Sedim. Res., v. A64, pp. 815-823.

DeCelles, P. G., Gehrels, G. E., Quade, J., Ojha, T. P., Kapp, P. A. and Upreti, B. N., 1998. Neogene foreland basin deposits, erosional unroofing, and the kinematic history of the Himalayan fold-thrust belt, western Nepal. Geol. Soc. Am. Bull., v. 110, pp. 2-21.

Department of Mines and Geology (DMG/HMGN), 1987, Geological Map of Far Western Nepal, 1:250,000.

Department of Mines and Geology (DMG/HMGN), 2003, Geological Map of Petroleum Exploration Block-2, Karnali, Far Western Nepal, 1:250,000

Dhital, M. R., Gajurel, A. P., Pathak, D., Paudel, L. P. and Kizaki, K. 1995, Geology and structure of the Siwaliks and Lesser Himalaya in the Surai Khola-Bardanda area, mid-western Nepal. Bull. Dept. Geol. Tribhuvan Univ., v. 4, pp. 1-70.

Dickinson, W. R. 1985, Interpreting detrital modes of greywacke and arkose. Jour. Sedim. Petrol., v.40, pp. 695-707.

Dickinson, W. R. and Suczek, C., 1979, Plate tectonics and sandstone compositions. Am. Assoc. Petrol. Geol. Bull., v. 63, pp. 2164-2182.

Dickinson, W. R., Beard, L. S., Brakenridge, G. R., Erjavec, J. L., Ferguson, R. C., Inman, K. F., Knepp, R. A., Lindberg, F. A. and Ryberg, P. T., 1983, Provenance of North American Phanerozoic sandstone in relation to tectonic setting. Geol. Soc. Am. Bull. v. 94, pp. 222–235.

Folk, R. L., 1980, Petrology of Sedimentary Rocks, Austin, Texas, Hemphills, 201p.

Gabriel, K. R., 1971, The biplot graphic display of matrices with application to principal component analysis. Biometrika v. 58, pp. 453–467.

Gansser, A., 1964, Geology of the Himalayas. Interscience, London, 289 p.

Garzanti, E., Ando′, S. and Scutella, M., 2000, Actualistic ophiolite provenance: the Cyprus case. Jour. Geol., v. 108, pp. 199–218.

Gautam, P. and Fujiwara, Y., 2000, Magnetic polarity stratigraphy of Siwalik Group sediments of the Karnali River section in western Nepal. Geophys. Jour. Int., v. 142, pp. 812-824.

Howard, J. L., 1994, A note on the use of statistics in reporting detrital clastic compositions. Sedimentology v. 41, pp. 747–753.

Huyghe, P., Galy, A., Mugnier, J. L. and France-Lanord, C., 2001, Propagation of the thrust system and erosion in the Lesser Himalaya: Geochemical and sedimentological evidence. Geology, v. 29, pp. 1007-1010.

Huyghe, P., Mugnier, J. L., Gajurel, A. P, and Decaillau, B., 2005, Tectonic and climatic control of the changes in the sedimentary record of the Karnali river section (Siwaliks of western Nepal). The Island Arc, v. 14, pp. 311-327.

Ingersoll, R. V., 1978. Petrofacies and petrologic evolution of the Late Cretaceous fore-arc basin, northern and central California. Jour. Geol., v. 86 (3), pp. 335–352.

Ingersoll, R. V. and Suczek C. A., 1979, Petrology and provenance of Neogene sand from Nicobar and Bengal fans. DSDP site 211 and 218. Jour. Sedim. Petrol., v. 49, pp. 1217-1228.

Ingersoll, R. V. and Eastmond, D. J., 2007, Composition of modern sand from the Sierra Nevada, California, U.S.A.: implications for actualistic petrofacies of continental-margin magmatic arcs: Journal of Sedimentary Research, v. 77, pp. 784-796.

Johnsson, M. J, 1993, The system controlling the composition of clastic sediments. In : Processes Controlling the Composition of Clastic Sediments (Ed. by M.J Johnsson and A. Basu), Spec. Pap. Geol. Soc. Am., v. 284, pp. 1-19.

Mugnier, J. L, Leturmy, P., Mascle, G., Huygle, P., Chalaron, E., Vidal, G., Husson, L. and Delcaillau, B., 1999, The Siwalik of Western Nepal: I. geometry and kinematics, Jour. Asian Earth Sci., v. 17 (5-6), pp. 629-642.

Mugnier, J. L., Delcaillau, B., Huyghe, P. and Leturmy, P., 1998, The break-back thrust splay of the Main Dun Thrust (Himalayas of western Nepal): evidence of an intermediate displacement scale between earthquake slip and finite geometry of thrust systems. Jour. Struct. Geol. v. 20, pp. 857-864.

Ohta, T. and Arai, H., 2007, Statistical empirical index of chemical weathering in igneous rocks: A new tool for evaluating the degree of weathering. Chemical Geology, v. 240, pp. 280–297.

Pettijohn, F. J., 1975, Sedimentary Rocks, 3rd ed. Harper & Row, New York, 628 p.

Pettijohn, F. J., Potter, P. E. and Siever, R., 1987. Sand and sandstone, 2nd ed. Springer-Verlag, 533 p.

Prins, M. A. and Weltje, G. J., 1999, End-member modeling of siliciclastic grain-size distributions: the late Quaternary record of eolian and fluvial sediment supply to the Arabian Sea and its paleoclimatic significance. In: Harbaugh, J. W., Watney, L., Rankey, E. C., Slingerland, R., Goldstein, R. H., Franseen, E. K. (Eds.), Numerical Experiments in Stratigraphy: Recent Advances in Stratigraphic/Sedimentologic Computer Simulations. SEPM Spec. Publ., v. 62, pp. 91– 111.

Robinson, D. M., DeCelles, P. G., Patchett, P. J. and Garzione, C. N., 2001, The kinematic evolution of the Nepalese Himalaya interpreted from εNd isotopes. Earth. Plant. Sci. Lett., v. 192, pp. 507-521.

Sigdel, A., Sakai T., Ulak, P. D., Gajurel A. P. and Upreti, B. N., 2011, Lithostratigraphy of the Siwalik Group, Karnali River section, far-west Nepal Himalaya. Jour. Nep. Geol. Soc. v. 43 (Spec. Issue), pp. 83-101.

Stattegger, K. and Morton, A. C., 1992, Statistical analysis of garnet compositions and lithostratigraphic correlation: Brent Group sandstones of the Oseberg field, northern North Sea. In: Morton, A.C., Hazeldine, R.S., Giles, M.R., Brown, S. (Eds.), Geology of the Brent Group. Geol. Soc. Spec. Publ., v. 61, pp. 245– 262.

Szulc, A. G., Najman, Y., Sinclair, H., Pringle, M., Bickle, M., Chapman, H., Garzanti, E., Ando, S., Huyghe, P.,Mugnier, J. L., Ojha, T. P. and DeCelles, P. G., 2006, Tectonic evolution of the Himalaya constrained by detrital $^{40}Ar/^{39}Ar$, Sm-Nd and petrographic data from the Siwalik foreland basin succession, SW Nepal. Basin Res., v. 18, pp. 375-391.

Tamrakar, N. K, Yokota, S. and Shrestha, S. D., 2003, Petrography of the Siwalik sandstones, Amlekhganj-Suparitar area, central Nepal Himalaya. Jour. Nep. Geol, Soc, v. 28. pp. 41-56.

Thio-Henestrosa, S. and Comas, M., 2011, CoDaPack v. 2 USER's GUIDE (http://ima.udg.edu/CoDaPack)

Tokuoka, T., Takayasu, K., Yoshida, M. and Hisatomi, K., 1986, The Churia (Siwalik) Group of Arung Khola area, west-central Nepal. Mem. Fac. Sci. Shimane Univ., v. 22, pp. 135-210.

Upreti, B. N. and Le Fort, P., 1999, Lesser Himalayan crystalline nappes of Nepal: problem of their origin. In: Macfarlane, A., Quade, J., and Sorkhabi, R. (eds.), Himalaya and Tibet: Mountain root to tops, Geol. Soc. Am., Spec. Pap., v. 328, pp. 225-238.

Van der Beek, P., Robert, X., Mugnier, J- L., Bernet, M., Huyghe, P. and Labrin, E., 2006, Late Miocene-Recent exhumation of central Himalaya and recycling in the foreland basin assessed by apatite fission track thermochronology of Siwalik sediments, Nepal. Basin Res. v. 18, pp. 413-434.

Von Eynatten, H., Barceló-Vidal, C. and Pawlowsky-Glahn, V., 2003, Modelling compositional change: the example of chemical weathering of granitoid rocks. Math. Geol. v. 35, pp. 231–251.

Weltje, G. J., 1994, Provenance and dispersal of sand-sized sediments: reconstruction of dispersal patterns and sources of sand-size sediments by means of inverse modeling techniques, PhD thesis, Geologicaa Ultraiectina.

Weltje, G. J., Meijer, X. D. and De Boer, P. L., 1998, Stratigraphic inversion of siliciclastic basin fills: a note on the distinction between supply signals resulting from tectonic and climatic forcing. In: Hovius, N., Leeder, M. (Eds.), Thematic Set on

Sediment Supply to Basins. Basin Res. v. 10, pp. 129– 153.

Weltje, G. J., 2002, Quantitative analysis of detrital modes: statistically rigorous confidence region in ternary diagrams and their use in sedimentary petrology. Earth Sci. Rev., v. 57, pp. 211–253.

Young, S. W., 1976, Petrographic textures of detrital polycrystalline quartz as an aid to interpreting crystalline source rocks. Jour. Sedim. Petrol., v. 46, pp. 595–603.

Zuffa, G. G., 1985, Optical analysis of arenites: influence of methodology on compositional results. In: Zuffa, G.G. (Ed.), Provenance of Arenites: North Atlantic Treaty Organization, Advanced Study Institute Series 148. Reidel, Dordrecht, pp. 165–189.